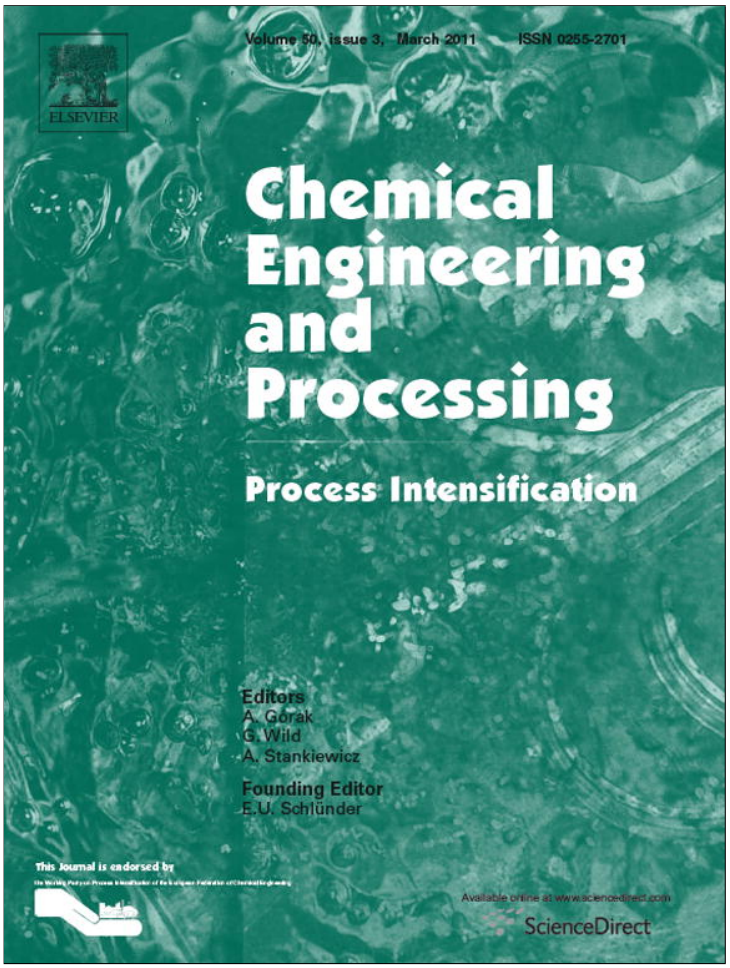

Chemical Engineering and Processing 50 (2011) 316–324

Contents lists available at ScienceDirect

Chemical Engineering and Processing: Process Intensification

journal homepage: www.elsevier.com/locate/cep

A coupling model for EGSB bioreactors: Hydrodynamics and anaerobic digestion processes

Mauren Fuentes[a,b,*], Nicolás J. Scenna[a,c], Pío A. Aguirre[a,d]

[a] INGAR - (CONICET-UTN), Avellaneda 3657 (3000) Santa Fe, Argentina
[b] Depto de Ciencias Básicas - UTN FRSF, Lavaise 610 (3000) Santa Fe, Argentina
[c] CAIMI-UTN FRR, Zeballos 1341 (2000) Rosario, Argentina
[d] Facultad de Ing. Qca, UNL, Santiago del Estero 2829 (3000) Santa Fe, Argentina

ARTICLE INFO

Article history:
Received 31 January 2010
Received in revised form 10 January 2011
Accepted 23 January 2011
Available online 1 February 2011

Keywords:
Dynamic modeling and simulation
Three-phase systems
EGSB reactors
Wastewater treatment

ABSTRACT

The aim of this paper is to present a coupling model for calculating both the hydrodynamic and anaerobic digestion processes in expanded granular sludge bed (EGSB) bioreactors for treating wastewaters. The bioreactor is modeled as a dynamic (gas–solid–liquid) three-phase system. An existing set of experimental data of three case studies based on the start-up and operational performance of EGSB reactors is used to adjust and validate the model. A novel parameter, the specific rate of granule rupture, is defined for calculating the biomass transport phenomena. Values around 1×10^{-20} dm d^2 g^{-1} are calculated for this parameter. Bioreactor performances were analyzed through the main variable profiles such as pH, COD, VFA and VSS concentration. A good agreement was obtained among experimental and predicted values. It seems to indicate that the proposed EGSB model is able to reproduce the main biological and hydrodynamic successes in the bioreactor.

1. Introduction

The expanded granular sludge bed (EGSB) reactor is a super high rate technology for wastewater treatment. It was introduced by De Man et al. [1] and has attained an increasing popularity in the last decade [2,3]. The conception of the EGSB reactor can be considered as an improvement of the upflow anaerobic sludge blanket (UASB) reactor developed by Lettinga et al. [3]. In the anaerobic digestion processes, complex organic substrates such as proteins, lipids, and carbohydrates are hydrolyzed into soluble amino acids, fatty acids, and sugars, followed by the fermentation to acetate, formate, hydrogen, and carbon dioxide which are finally utilized by methanogenic microorganism to form methane [4–6].

Both EGSB and UASB are based on the ability of microorganism to form dense aggregates by autoimmobilization. However, inside the EGSB reactor, the higher upflow velocities, which are caused by a high recycle rate and a high height/diameter ratio, cause the sludge expansion through the whole reactor thus improving its contact with the effluent and reduce the unit dead volume [7,8]. Since higher organic loading rates (up to 40 kg of chemical oxygen demand COD m^{-3} d^{-1}) can be accommodated in EGSB, the gas production is also higher, improving even more the mixing inside the reactor.

The exact mixing pattern cannot be generalized, and it must be evaluated in each reactor by assessing the reactor hydrodynamics [9]. However, a fully expanded EGSB reactor can be considered as a completely mixed tank [10,11], and liquid film mass transfer resistance seems to be negligible [12]. The knowledge of the bed expansion plays an important role in the design and operation of an EGSB reactor, because it is the key point to reach a compromise between bed expansion and sludge washout, and the stability and performance of the EGSB system would be sensitive to the degree of expansion [13].

Some ideas from solid dynamics in a three-phase fluidized bed reactor can be used to describe the multiple solid–liquid–gas interactions that take place in EGSB reactors. In previous works, a heterogeneous model for three-phase anaerobic fluidized bed (AFB) reactors was developed and validated [14–16]. The aim of this work is to apply this methodology for modeling EGSB reactors. Thus, a heterogeneous model for EGSB bioreactors is presented here. This modeling approach combines the dynamics of the three phases present in the reactor including biochemical, physico-chemical and hydrodynamic processes. Several details of reactor design, sludge and wastewater characteristics, and operational conditions are required for model adjustment and validation. Almost all works published describe better the biochemical performance of EGSB reactors than their hydrodynamics. Due to the lack of information on some parameters that can be measured and are

* Corresponding author at: INGAR - Instituto de Desarrollo y Diseño- Avellaneda 3657 (3000) Santa Fe, Argentina. Tel.: +54 342 4534451; fax: +54 342 4553439.
E-mail address: mfuentes@santafe-conicet.gov.ar (M. Fuentes).

0255-2701/$ – see front matter © 2011 Elsevier B.V. All rights reserved.
doi:10.1016/j.cep.2011.01.005

not reported, the authors should solve the initialization problem via simulation, i.e. a sensitivity analysis of model results related to these parameters is required.

The paper is organized as follows: in Section 2, main mathematical equations of the global model are presented, and some hypotheses related to the bioparticle model and hydrodynamics are discussed. Computational aspects of model implementation and solution using gPROMS are described in Section 3. Model adjustment and validation using an existing set of experimental data of case studies based on the start-up and operational performance of EGSB reactors is presented in Section 4. Finally, conclusions are drawn in Section 5.

2. Mathematical model

As mentioned, the EGSB is modeled as a three-phase gas–solid–liquid system. The solid phase consists of bioparticles (granules) composed by active and non-active biomass. The liquid phase is composed by the chemical species in solution (substrates, products, enzymes, ions, and water) and (active and non-active) single suspended cells, which are assumed to behave as solutes. The gas phase is formed by the gaseous products from degradation stages.

The global EGSB model results analogous to the AFB reactor model previously published [14–16]. The main subsystem models are: (1) the anaerobic digestion model; (2) the bioparticle model; and (3) the hydrodynamics model. Since the main differences between both technologies are based on characteristics of the solid phase and hydrodynamics, the paper is essentially oriented to discuss these aspects. Some hypotheses and the main mathematical equations have been rewritten for better comprehension.

2.1. Anaerobic digestion model

The anaerobic digestion model involves the biochemical (growth-uptake, death, hydrolysis and disaggregating) and physico-chemical (system charge balance for calculating pH, gas–liquid mass transfer) processes which take place in the bioreactor. All terms related with mass transfer processes, model parameters and constants have been previously described [9,14–16]. However, the main rate expressions $\left(\sum_j R_{ik}^j + \sum_j T_{ik}^j\right)$ are summarized in Table A.1 of Appendix A.

A novel aspect in the EGSB model is related to modeling the disaggregation of single suspended cells from biomass granules. For modeling the disintegration of aggregates, some physical aspects related to the structure and compactness of granules need to be considered. Hydrodynamics affects biomass processes inside a bioreactor. These effects are more pronounced in fluidized beds than in granular sludge bed reactors, attending to the operational fluid velocity ranges [7,17].

Tiwari et al. [18] studied the influence of some factors such as temperature, alkalinity, nature and strength of substrate, and cation concentration on granule formation in sludge bed reactors. They concluded that: (1) a careful temperature control and an adequate alkalinity is required for generation and maintenance of granules; (2) the nature and strength of substrate in conjunction with intragranular diffusion to a large extent determines the microstructure of the granules; and (3) the divalent cations such as calcium and iron may enhance granulation by ionic bridging and linking exocellular polymers. However, their presence in excess may lead to cementation due to precipitation leading to increased ash content and mass transfer limitation.

In this work, the parameter specific rate of granule rupture k_r has been defined for calculating the biomass transport phenomena. This parameter explains how the process of granulation is affected by all these environmental and operational conditions, and differs of the specific rate of biomass hydrolysis, which is related to the enzyme attack on non-active biomass. Since several factors are involved in the stability and formation of granule, and no other modeling approach has been published, the rate of granule (disaggregating) rupture is modeled as a first-order function on the energy dissipation parameter ω (which is an upflow velocity function, $\omega = U_o(-\partial p/\partial z)$, $\partial p/\partial z = -g\sum_k \varepsilon_k \rho_k$), and mass concentration of each microbial species present in the biomass aggregates (see Table A.1):

$$r_{r_i} = \varepsilon_S k_r \omega X_i^S \quad (1)$$

Parameter k_r has been assumed the same for all biological species. A sensitivity analysis of model results related to this parameter is presented in Section 4.

2.2. Bioparticle model

Generally, the granule composition has been described from the ash content, moisture and (active and non-active) biomass fraction. These parameters can vary during the granule formation, and thus, the dry density of granules varies. As a first modeling approach, homogeneous biomass distribution on granules, constant wet biomass density and spherical geometry are assumed. No mass transfer limitations in the granule and the liquid bulk are assumed. The substrate concentration has the same value throughout the bioparticle.

For making the model workable, a simplifying assumption on granule diameter d_{bp} is considered. A simple relationship dealing with the net biomass growth-decay-hydrolysis-disaggregating rate is used to calculate the "average" granule diameter as a time function [19]:

$$d\frac{d_{bp}}{dt} = \frac{2}{\pi d_{bp}^2} d\frac{V_{bp}}{dt} = \frac{2}{\pi d_{bp}^2} \frac{V\left(\sum_{i,j} R_{iS}^j + \sum_{i,j} T_{iS}^j\right)}{N_{bp}\rho_s(1 - AC_{bp}/100)(1 - MC_{bp}/100)} \quad (2)$$

The number of bioparticles N_{bp} in the control volume (V) can be expressed by dividing the total sludge volume (V_S) by the average volume of one aggregate (V_{bp}):

$$N_{bp} = \frac{V_S}{V_{bp}} = \frac{V\varepsilon_S X_T^S}{\rho_S(1 - AC_{bp}/100)(1 - MC_{bp}/100)} \frac{6}{\pi d_{bp}^3} \quad (3)$$

Substituting Eq. (3) into Eq. (2), time variation of granule diameter can be calculated as:

$$d\frac{d_{bp}}{dt} = \frac{d_{bp}}{3} \frac{\left(\sum_{i,j} R_{iS}^j + \sum_{i,j} T_{iS}^j\right)}{\varepsilon_S X_T^S} \quad (4)$$

where X_T^S is the total concentration of biological species in the solid phase $\left(\sum_i (X_{ia}^S + X_{ina}^S)\right)$.

2.3. Hydrodynamics model

Characteristics of phase mixture and flow patterns are expressed by the hydrodynamic model. Since the EGSB is assumed

Table 1
Details of experimental studies used in the adjustment and validation of the model.

Parameter (dimension)/case study[a]	R1			R2			R3
Reactor design							
Working reactor volume (dm^3)	1.3			157.5			0.48
Inner diameter (dm)	0.53			2			0.418
Height of the water level (dm)	6.2			50			3.53
Sludge characteristics							
Biomass concent. (Gvss dm^{-3})	43.4			4.6			117
Initial load (dm^3)	0.23			nd			0.09
Ash content (%)	19			nd			nd
Moisture content (%)	94.8			nd			nd
Granule mean diameter (10^2 dm)	2.3 ± 0.2			nd (2.3)			1.6
Granule density (g dm^{-3})	1026			nd (1026)			nd (1026)
Steps (disturbances)	I	II	III	I	II	III	I
Time horizon/step (d)	28	30	20	113	92	124	nd
Wastewater characteristics							
Influent TCOD (mg dm^{-3})	444 ± 51	444 ± 51	444 ± 51	126 ± 53	180 ± 0.150	156 ± 48	1280
Influent SCOD (mg dm^{-3})	nd, 26 ± 2 as S_{HAc}	nd	nd	56 ± 22	79 ± 31	55 ± 19	1280
Influent VSS (mg dm^{-3})	75 ± 36	75 ± 36	75 ± 36	42 ± 27	54 ± 29	63 ± 30	0
Influent pH	8.9 ± 0.4	8.9 ± 0.4	8.9 ± 0.4	6.9 ± 0.1	6.7 ± 0.2	6.9 ± 0.2	7
Substrate composition (%COD)[b]	X_{CH}–X_P–X_{Li}–S_{HAc}: 39–44–11–6			X^L–X_{CH}–X_P–S_{HAc}: 29–9–11–51			S_{HAc}: 100
Operational characteristics							
Temperature (°C)	30 ± 2.0	30 ± 2.0	30 ± 2.0	29.7 ± 1.7	30.3 ± 2.0	32 ± 1.9	24
HRT (d)	0.33	0.25	0.17	0.17	0.17	0.17	0.07
OLR (gCOD dm^{-3} d^{-1})	1.33	1.78	2.66	0.64	0.92	0.80	18.29
Biomass concent. (gVSS dm^{-3})	10.00	10.06	10.43	6.4	9.2	8.0	19
Hydrodynamic characteristics							
Static bed height (dm)	nd (2.48)			nd (12.06)			0.66
Bed porosity (dm^3 dm^{-3})	nd (0.4)			nd (0.4)			0.4
Influent flow rate (dm^3 d^{-1})	3.89	5.21	7.78	945	945	945	6.85
Liquid upflow velocity (dm d^{-1})	2568	1968	2353	300	600	900	4800
Recycle flow rate (dm^3 d^{-1})	563	429	511	0	945	1890	652

[a] R1-Veronez et al. [28], R2-Kato et al. [29], R3-Brito and Melo [12]. The assumed values are written between parentheses.
[b] See section nomenclature for notation.

to behave as a continuous stirred tank reactor due to the effects of the high recirculation rate, a completely mixed flow pattern is considered.

In EGSB reactors, the bed expansion is closely related to the settling characteristics of the sludge. Almost all works published suggest that the mean settling velocity of the granules is in accordance with Stoke's law because the settling process is in the laminar flow range [20–22], whilst others suggest that it is in accordance with the Allen formula because the settling process falls within the intermediate flow range [23]. However, the settling characteristics of the granules have scarcely been discussed theoretically by the above workers.

Liu et al. [11] proposed the Eq. (5) for calculating the EGS bed height assuming that the settling process of the granules is in the category of intermediate flow regime. The authors used the well known Richardson and Zaki [24] correlations to calculate the bed expansion, the expansion coefficient (n) and the terminal settling velocity (U_t). This approach is in accordance with the mathematical statement of the generalized bubble and wake model (GBWM [25]) selected here to describe the three-phase system. GBWM equations for calculating fluidization characteristics (phase holdup and superficial velocity) are summarized in Table B.1 of Appendix B.

From the definition of bed expansion, using the flow equation, and making mathematical transformations, the bed height can be calculated as [11]:

$$H = H_0 \left(1 + \frac{e^{(\ln U_0/U_t)/n} - \varepsilon_0}{1 - e^{(\ln U_0/U_t)/n}}\right) \quad (5)$$

Since parameters U_t and n are functions of biomass concentration (see Table B.1), the bed height is also a biomass function. Properties H_o and ε_o are calculated at the static bed condition.

Biochemical processes are assumed to occur only in the expanded granular sludge zone. As the bed height is a time function, the control volume assumed to compute the differential and algebraic equation (DAE) system varies. Mass balance equations for phase components are described in Table B.1 of Appendix B.

3. Computational aspects

The mathematical model was implemented and solved using the process modeling software tool gPROMS (Process Systems Enterprise Ltd.). A "high-index" DAE system (index > 1) was verified [26,27]. Low steady state concentration values are considered as initial values for the biological and chemical species. In all case studies, 68% of total non-active biomass, 6% for active acidogens (X_{GL}, X_{AA}) and methanogens (X_{Ac}), and 2.8% for the other active species are assumed. The total CPU time required to solve case studies described in the following section is about 7 s on an 800 MHz Pentium IV PC.

4. Results and discussion

4.1. Case studies

An existing set of experimental data obtained by Veronez et al. [28], Kato et al. [29] and Brito and Melo [12], based on the start-up and operational performance of EGSB reactors, is used here to adjust and validate the proposed model. By simplicity, the case studies have been named as R1, R2 and R3, respectively. Details of reactor design, sludge and wastewater characteristics, and operational conditions are summarized in Table 1.

4.2. Model adjustment

There are two types of parameters that have to be calculated for model adjustment: (1) parameters that can be measured and are not reported in the original sources; and (2) empirical parameters related to kinetics and biomass transport in EGSB reactors. As

Table 2
Experimental and predicted values of the effluent stream for R1 [28].

Step	pH		Total COD (mg dm^{-3})		Soluble COD (mg dm^{-3})		VFA (mgHAc dm^{-3})		VSS (mg dm^{-3})	
	Exp.	Mod.	Exp.	Mod.	Exp.	Mod.	Exp.	Mod.	Exp.	Mod.
I	7.0 ± 0.1	6.89	119 ± 15	117	98 ± 16	93	16 ± 2	19	19 ± 6	19
II	6.9 ± 0.2	6.91	143 ± 25	136	106 ± 10	103	16 ± 1	25	35 ± 9	29
III	7.7 ± 0.1	7.75	181 ± 40	190	130 ± 25	112	23 ± 1	29	32 ± 9	69

Table 3
Experimental and predicted values of the effluent stream for R2 [29].

Step	pH		Total COD (mg dm^{-3})		Soluble COD (mg dm^{-3})		VFA (mgHAc dm^{-3})		VSS (mg dm^{-3})	
	Exp.	Mod.	Exp.	Mod.	Exp.	Mod.	Exp.	Mod.	Exp.	Mod.
I	nd	6.90	68 ± 29	67	42 ± 21	36	nd	19	13 ± 8	22
II	nd	6.73	87 ± 21	84	55 ± 22	44	nd	21	8 ± 3	29
III	nd	6.87	79 ± 26	86	44 ± 15	44	nd	20	24 ± 17	30

mentioned, the lack of information on granule characteristics and static bed conditions requires a sensitivity analysis of model results to calculate these parameters and make the model workable. The values finally assumed are written between parentheses in Table 1. Some aspects on the influence of these parameters are discussed at the end of Section 4.3.

Here the interest is focused in calculating the empirical parameters. Only the novel parameter specific rate of granule rupture (k_r) is estimated via simulation, and no other biochemical and physico-chemical parameters are modified. The procedure consists in an iterative calculation of model variables changing the k_r value.

Arbitrarily, the first case study (R1) was selected to adjust the model. Bioreactor R1 was used for treating a synthetic wastewater with a mean COD concentration of 444 mg dm^{-3}, basically composed by carbohydrates (sucrose, starch and cellulose), proteins (meat extract) and lipids (soy oil) [28]. A commercial detergent was used to emulsify the lipid. The experimental setup consisted in three stepped disturbances in the organic loading rate (OLR) by increasing the feed flow rate, keeping the same influent COD concentration (Table 1).

Fig. 1 shows the sensitivity analysis of model results related to k_r for R1. An initial value of 1×10^{-22} dm d^2 g^{-1} ($k_r g = 7.3 \times 10^{-11}$ dm^2 g^{-1}, see Eq. (1)) was used, and values up to 200 k_r were evaluated. An increase in the parameter k_r causes a decrease in the granule mean diameter and solid holdup; the

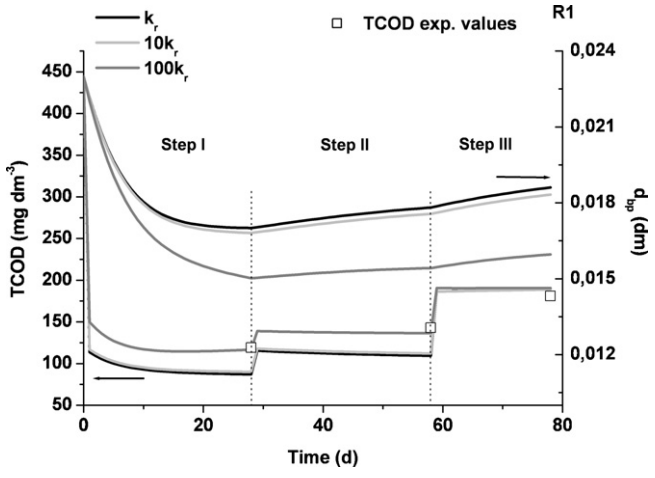

Fig. 1. Sensitivity analysis of model results related to the specific rate of granule rupture (k_r).

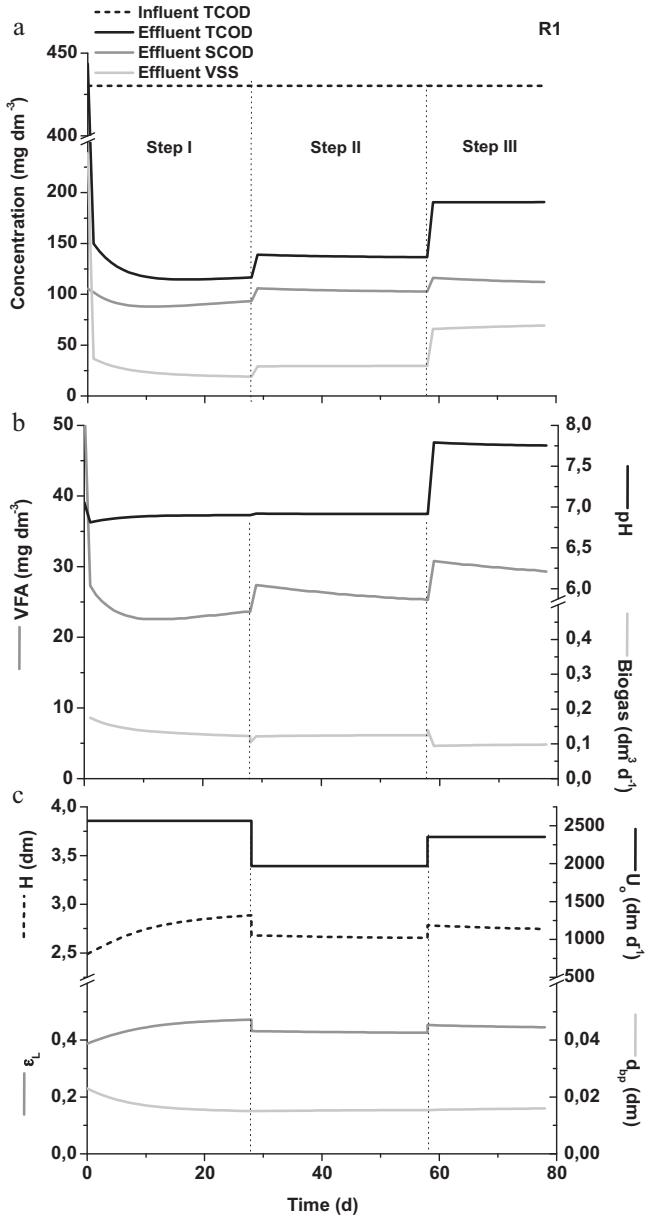

Fig. 2. R1 simulation results: (a) TCOD, SCOD and VSS concentration values; (b) VFA (as acetate) concentration, biogas flow rate and pH; and (c) bed height, liquid holdup, liquid upflow velocity and granule diameter.

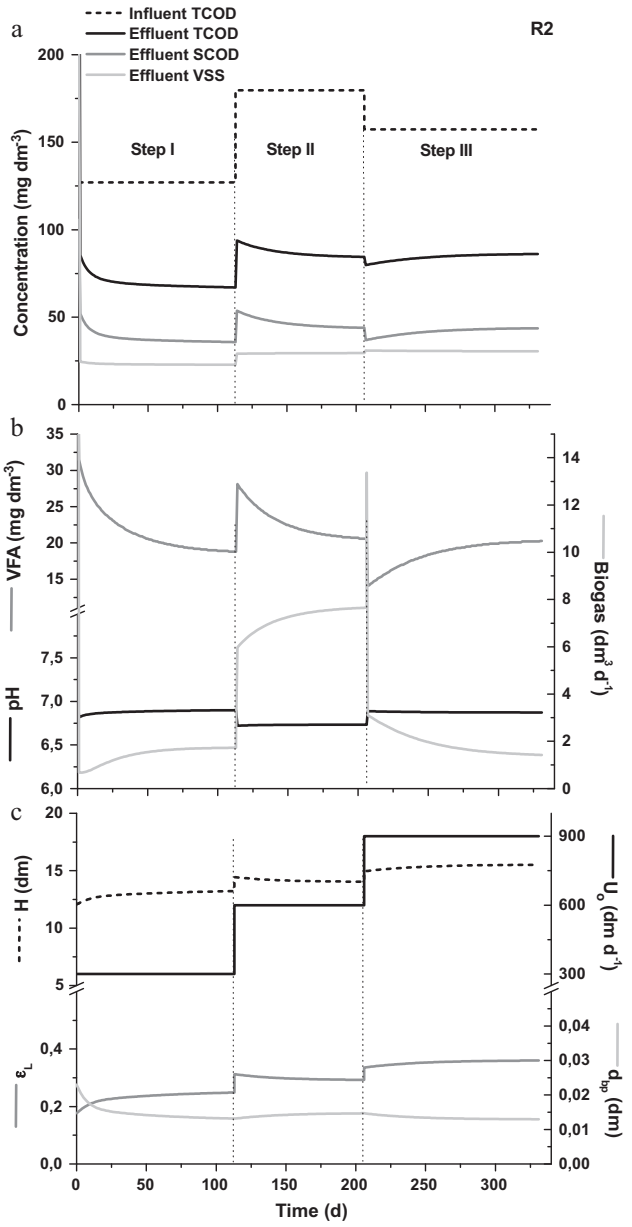

Fig. 3. R2 simulation results: (a) TCOD, SCOD and VSS concentration values; (b) VFA (as acetate) concentration, biogas flow rate and pH; and (c) bed height, liquid holdup, liquid upflow velocity and granule diameter.

terminal settling velocity decreases and thus, an increase in the height of reactor is verified. In practice, the total COD concentration in the effluent stream increases due to a higher concentration of single suspended cells, and small granules can leave the bioreactor.

As observed in Fig. 1, a good agreement between experimental and predicted values of total COD at steady state conditions is obtained for a value around 100 k_r (1×10^{-20} dm d^2 g^{-1}). Model responses for the COD concentration and other main macroscopic variables such as volatile suspended solids (VSS), volatile fatty acids (VFA, as acetate), biogas flow rate and pH, are depicted in Fig. 2. The vertical dotted lines indicate the time duration of each step-type disturbances.

Table 2 shows a comparison between experimental and predicted values measured at the end of each step-type disturbance. A height of 2.48 dm (40% of the maximum height) and bed porosity equal to 0.4 were assumed for calculating the static bed condition.

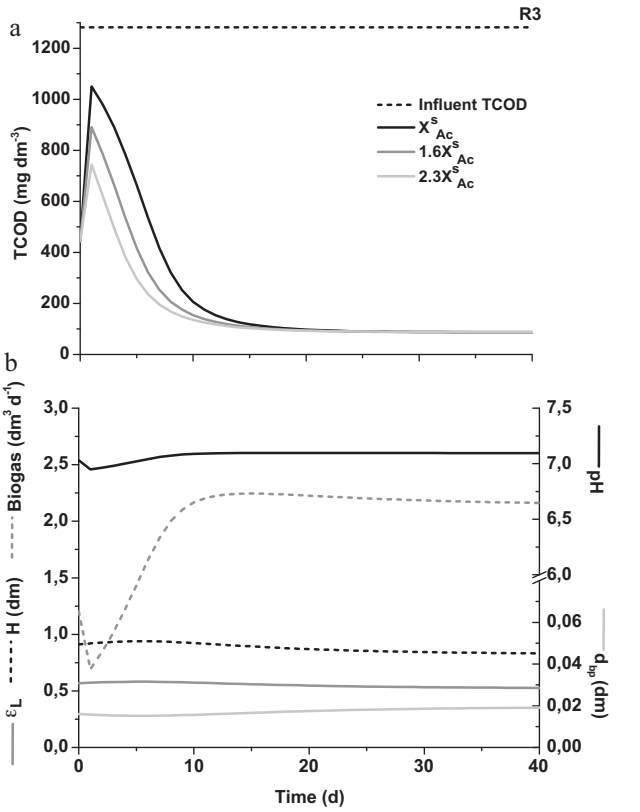

Fig. 4. R3 simulation results: (a) TCOD concentration for different initial conditions; and (b) biogas flow rate, pH, bed height, liquid holdup and granule diameter.

4.3. Model validation

Case studies R2 an R3 are used for model validation. Simulation results are depicted in Figs. 3 and 4, respectively. Tables 3 and 4 show a comparison between predicted and experimental data for each case. As mentioned, the simulated values were measured at the end of each step-type disturbance. Model parameters were not modified, i.e. they are the same as used in case R1.

R2 experience was carried out in a pilot EGSB reactor fed with the effluent from a full-scale UASB treating municipal wastewater [29]. The bioreactor was monitored in three different periods by varying the upflow velocity according to Table 1. Values of 30, 30, 0, and 40%VSS were assumed to model carbohydrate, protein, lipid and suspended biomass composition in the influent stream, respectively. Soluble COD was measured as acetic acid concentration.

During the first step-type disturbance, bioreactor R2 operated with a UASB configuration (recirculation flow equal to zero). Simulation values resulted also appropriate for this stage (Fig. 3), although a completely mixed flow pattern was considered. However, the authors do not recommend using this model for UASB units.

The original research in the case study R3 was focused on the feasibility of EGSB reactors for the treatment of low strength soluble wastewaters; acetic acid was used as substrate. Authors [12] conducted a study of the substrate concentration profile in the bioreactor and concluded that the EGSB mixing properties approach those of an ideal continuous stirred tank reactor. Fig. 1 in the original source [12] shows that the acetic acid concentration at the reactor inlet is 770 mg dm^{-3} and immediately falls down to 70 mg dm^{-3} at the reactor dimensionless length equal to 0.01.

In Section 3 are described the initial conditions assumed to calculate the biomass composition in the granule. Same values were assumed for all case studies; however, the total biomass concen-

Table 4
Experimental and predicted values of the effluent stream for R3 [12].

Step	pH		Total COD (mg dm^{-3})		Soluble COD (mg dm^{-3})		VFA (mgHAc dm^{-3})		VSS (mg dm^{-3})	
	Exp.	Mod.	Exp.	Mod.	Exp.	Mod.	Exp.	Mod.	Exp.	Mod.
I	7.0 ± 0.2	7.09	nd	87	nd	74	70	70	nd	14

Table A.1
Homogeneous reaction rates (R) and mass transfer and transport process rates (T) for phase components[a].

ϕ_{ik}	$\sum_j R_{ik}^j + \sum_j T_{ik}^j$	i
$X_{i_a}^S$	$\varepsilon_S[\mu_i X_{i_a}^S - k_{d_i} X_{i_a}^S - k_r \omega X_{i_a}^S]$	16–23
$X_{i_{na}}^S$	$\varepsilon_S[k_{d_i} X_{i_a}^S - k_{bh} X_{i_{na}}^S - k_r \omega X_{i_{na}}^S]$	16–23
$X_{i_a}^L$	$\varepsilon_L[\mu_i X_{i_a}^L - k_{d_i} X_{i_a}^L] + \varepsilon_S k_r \omega X_{i_a}^S$	16–23
$X_{i_{na}}^L$	$\varepsilon_L[k_{d_i} X_{i_a}^L - k_{bh} X_{i_{na}}^L] + \varepsilon_S k_r \omega X_{i_{na}}^S$	16–23
X_i	$\sum_{j=1-2} \nu_{i,j} k_{Hid,j} \varepsilon_L X_j$	11–15
S_i	$\sum_{j=3-10} \nu_{i,j} \mu_j (\varepsilon_S X_{j_a}^S + \varepsilon_L X_{j_a}^L) + \sum_{j=1-2} \nu_{i,j} k_{Hid,j} \varepsilon_L X_j + \sum_{j=1-2} f_{bio,i} \nu_{i,j} k_{Hid,j} \times \sum_{j=11-18} (\varepsilon_S X_{j_{na}}^S + \varepsilon_L X_{j_{na}}^L)$	1–7,10
S_i	$\sum_{j=3-10} \nu_{i,j} \mu_j (\varepsilon_S X_{j_a}^S + \varepsilon_L X_{j_a}^L) - \varepsilon_L (k_L a)_i (S_i - I_{COD} K_{H,i} p_{gas,i})$	8–9
E_i	$\sum_{j=4-5} \nu_{i,j} \mu_j (\varepsilon_S X_{j_a}^S + \varepsilon_L X_{j_a}^L) - k_{de,i} E_i$	24–25
$p_{gas,i}$	$\nu_{st} p_{gas,T} \varepsilon_L (k_L a)_i (S_i / I_{COD} - K_{H,i} p_{gas,i})$	8–9

[a] See Appendix C for notation.

tration and substrate composition vary. It explains the decrease in the granule mean diameter at the beginning of the reactor start-up. The concentration of some biological species decreases when the substrate composition results insufficient, and the net biomass growth-decay-hydrolysis-disaggregating rate is negative. At the same time, when the substrate is rich in a specific metabolite and the initial concentration of the degrader species increases, the consumption (uptake) rate increases although steady state conditions are reached at the same time (Fig. 4).

Although the original sources are not oriented to analyze the hydrodynamic performance of EGSB bioreactors, the main hydrodynamic variables for R1, R2 and R3, have been added in Figs. 2(c), 3(c) and 4(b), respectively. Since the gas holdup in anaerobic reactors is less than 0.03, changes in the bed porosity can be examined from the liquid holdup (ε_L) variations. Sudden changes in the liquid upflow velocity (U_o) cause variations in the liquid holdup and thus, in the bed height profile. As observed, these events are more marked than those caused by biological processes.

As an example, the case study R3 is selected to show a sensitivity analysis of model results related to some parameters that were assumed to carry out the simulation. Fig. 5 shows the bioreactor performance for different initial values of bed height (H_o) keeping the same initial biomass concentration. For a value equivalent to $2H_o$, a double amount of biomass is present in the reactor, and the COD removal rate increases during the first days. Contrarily, for

Table A.2
Variables (i) and processes (j) taken into account in the anaerobic digestion model[a].

Variable	Description	i	Processes	j
X_{CH}	Carbohydrate	11	Carbohydrate hydrolysis	1
X_P	Protein	12	Protein hydrolysis	2
X_{Li}	Lipid	13	Lipid hydrolysis/glycerol uptake	3
X_{I-CH}	Inert carbohydrate	14	Glucose uptake	4
X_{I-P}	Inert protein	15	Amino acid uptake	5
S_{GI}	Glucose	1	LCFA uptake	6
S_{AA}	Amino acid	2	Valerate uptake	7
S_{LCFA}	LCFA	3	Butyrate uptake	8
S_{HVa}	Valerate	4	Propionate uptake	9
S_{HBu}	Butyrate	5	Acetate uptake	10
S_{HPr}	Propionate	6	X_{Glic} decay	11
S_{HAc}	Acetate	7	X_{GL} decay	12
S_{CH4}	Methane	8	X_{AA} decay	13
S_{IC}	Inorganic carbon	9	X_{LCFA} decay	14
S_{IN}	Inorganic nitrogen	10	X_{Va} decay	15
X_{bio}	Biomass	16–23	X_{Bu} decay	16
E_{CH}	Enzymes in process $j=1$	24	X_{Pr} decay	17
E_P	Enzymes in process $j=2$	25	X_{Ac} decay	18
			CH_4 mass transfer	T8
			CO_2 mass transfer	T9

[a] Mass balances are expressed in grams of chemical oxygen demand per liter per day (g COD L^{-1} d^{-1}), except for inorganic carbon and nitrogen (mol L^{-1} d^{-1}), gas phase components (atm L^{-1} d^{-1}) and enzymes (AU L^{-1} d^{-1}). Enzymatic activity is measured in Anson Unit (AU).

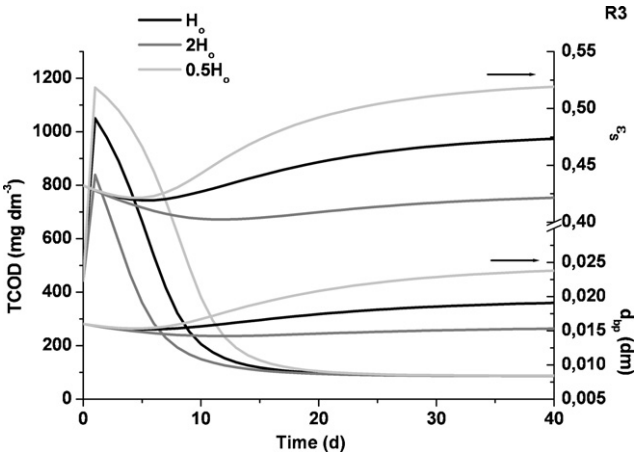

Fig. 5. Sensitivity analysis of model results related to the initial value of bed height (H_o) for R3.

initial values less than H_o, the bioreactor efficiency decreases. However, the time to reach the steady state conditions and the effluent COD values are the same for all cases.

At less bed height, the OLR increases for the same feed flow rate, and a high biomass concentration is obtained in the reactor. In Fig. 5, higher values of solid holdup and granule mean diameter are observed for this condition.

In general, the granular diameter ranges between 0.5 and 5 mm, but the mean diameter of sludge granules in full-scale installations typically ranges between 1 and 3 mm. On the other hand, larger sludge granules have low density whose values range between 1000 and 1050 g dm^{-3} [11]. The effects of granule mean diameter are depicted in Fig. 6; the same sludge density and initial biomass concentration are considered.

Experimental data on hydrodynamic behavior of EGSB reactors attending to settling characteristics of granules is scarcely. Bioparticles with less mean diameter are assumed to be fluidized in higher extension having a less terminal settling velocity. Thus, a higher bed expansion is predicted for granules of 1.6 mm when compared with granules of 2.3 mm (Fig. 6). The solid holdup, bed height and biomass concentration varies so that the total biomass results the same in both cases and a similar profile is obtained for total COD values. The risk of working with small bioparticles is the biomass washout when high upflow velocities are applied for bed expansion.

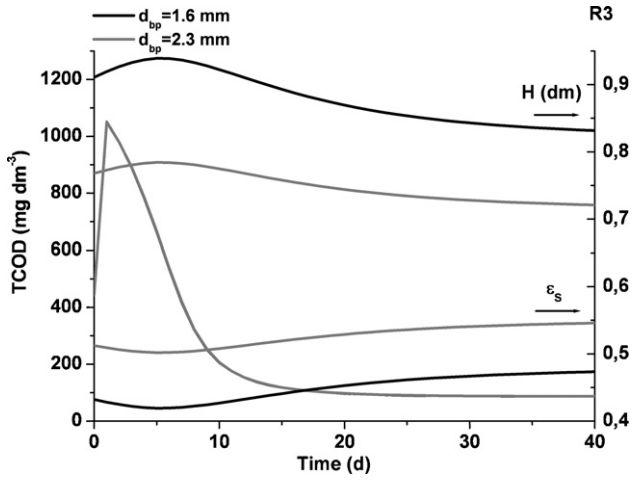

Fig. 6. Sensitivity analysis of model results related to the initial value of granule mean diameter (d_{bp}) for R3.

5. Conclusions

A dynamic model was proposed and adjusted to simultaneously compute the dynamics of the phases and their components in an expanded sludge bed reactor. Three case studies were investigated; bioreactor performances were analyzed through the main variable profiles such as pH, COD, VFA and VSS concentration. Since the information on sludge characteristics and static bed condition is incomplete, some values had to be assumed after a sensitivity analysis. Based on the results obtained during this study, the following conclusions can be drawn:

(1) The EGSB model can be adjusted by calculating the specific rate of granule rupture, without modifying any other parameter. A value of 1×10^{-20} dm d^2 g^{-1} was obtained via simulation. An increase in this parameter predicts a decrease in the COD removal efficiency caused by a higher concentration of single suspended cells.
(2) A sensitivity analysis of model results related to the static bed height and bioparticle diameter, showed the interaction between hydrodynamic events and biological performance of the bioreactor. The former modifies the COD removal rate during the first days of the reactor start-up but the time to reach the steady state conditions and COD values are the same for all cases. On the other hand, an increase in the granule diameter causes a decrease in the bed expansion, although the COD profile does not vary for the same biomass initial conditions.
(3) In general, model predictions agree satisfactorily with the experimental observations obtained during the start-up policies of bioreactors. It seems to indicate that the EGSB model, based on the anaerobic degradation scheme proposed by Angelidaki et al. and the GBW model to explain the hydrodynamic behavior of reactor, is able to reproduce the main successes of bioreactor.
(4) The EGSB model allows predicting profiles of non-macroscopic variables such as substrates and biological species concentration. Thus, additional information of the investigated system can be obtained. The model is able to resist strong numerical disturbances to represent a "step by step" start up of the reactor.

Acknowledgements

The authors acknowledge financial support from Consejo Nacional de Investigaciones Científicas y Técnicas (CONICET), Agencia Nacional para la Promoción de la Ciencia y la Tecnología (ANPCyT) and Universidad Nacional del Litoral of Argentina.

Appendix A.

A.1. Biochemical and physico-chemical processes

The anaerobic digestion model proposed by Angelidaki et al. [4] is selected here to represent the degradation scheme. The model involves two enzymatic processes: hydrolysis of (a) undissolved carbohydrates and (b) undissolved proteins, and eight microorganism trophic groups: (1) glucose-fermenting acidogens; (2) lipolytic bacteria-acidogenesis from glycerol combined with lipid (triglyceride) hydrolysis-; (3) long-chain fatty acid (LCFA)-degrading acetogens; (4) amino acid-degrading acidogens; (5) propionate-; (6) butyrate-; and (7) valerate-degrading acetogens; and finally (8) aceticlastic methanogens. This selection is sustained by previous results on model application and simplicity of the biomass model, and hydrogen stoichiometry [30,31]. The hydrolysis model proposed by Fuentes et al. [16] is used to represent the enzymatic processes of biopolymers.

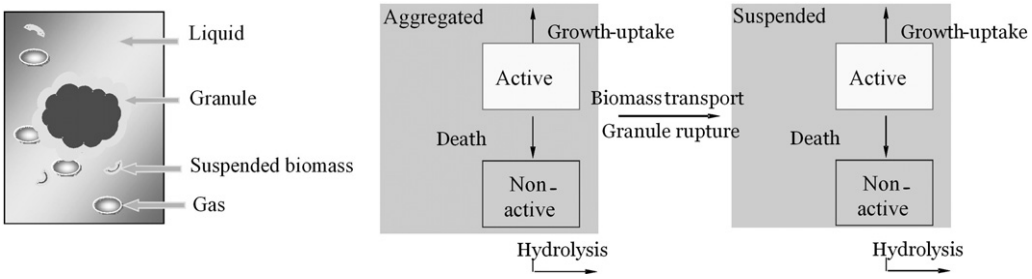

Fig. A.1. Biochemical processes and interaction between aggregated and suspended biomass.

Fig. A.1 shows a schematic representation of the interaction between aggregated and suspended biomass involving the growth-uptake, death, hydrolysis and disaggregating processes. Mathematical relationships on reaction and mass transfer process rates are summarized in Table A.1. Variables (i) and processes (j) taken into account in the anaerobic digestion model are described in Table A.2.

In Table A.1, biological species numeration (i = 16–23) has been extended to suspended single cells and aggregated biomass of the same (active and non-active) species i. The specific growth and death rates are assumed to be the same for suspended and aggregated biomass. Non-active biomass is considered as particulate material subjected to hydrolysis. Aspects related to the novel parameter specific rate of granule rupture k_r, were discussed in Section 2.1.

Equilibrium in solution model involves mass balance equations for total concentration of LCFA, volatile fatty acids (acetic, propionic, butyric and valeric), inorganic carbon, inorganic nitrogen, phosphate, "other anions", and "other cations". The relationships of the acid–base equilibrium model and temperature dependence are taken from Batstone et al. [32].

The liquid–gas mass transfer is modeled assuming ideal gas behavior, and constant total gas phase pressure. The mass balance for gas phase components (methane, carbon dioxide and water vapor) is expressed as a function of its partial pressure (Table A.1). Water vapor pressure is calculated by an Antoine-type equation. The gas–liquid mass transfer coefficient (k_La) varies a great deal depending on mixing, temperature and liquid properties; for simplicity and as recommended by Batstone et al. [32], the same k_La value is used for all gases.

Biochemical rate equation matrixes, kinetic and physico-chemical parameters are described in the original sources [4,14–16,30–32].

Appendix B.

B.1. Generalized bubble and wake model (GBWM)

The wake concept considers the three phase expanded bed to be composed of: (1) the gas bubble region; (2) the wake region; and (3) the solid–liquid fluidization region. The porosity in the solid–liquid fluidization region can be expressed by the Richardson and Zaki [24] equation, the wake region moves at the same velocity as the bubble, and the porosity of this region can be different as the solid–liquid fluidization one. The simplified wake theory, i.e. the liquid wakes are particle free, is used to calculate the liquid holdup [33]. Table B.1 summarizes the mathematical equations to calculate fluidization characteristics.

A constant volumetric flow through the fluidized bed is assumed, the velocity in the bed cross section is approximately

Table B.1
GBWM equations to calculate fluidization characteristics and mass balance equations for phase components.

GBW Model	
Liquid phase	
Holdup	$\varepsilon_L = \left[\frac{U_l}{U_t} - k\frac{U_g}{U_t}\right]^{1/n}[1-\varepsilon_G - k\varepsilon_G]^{1-1/n} + k\varepsilon_G, \quad k = 3.5\varepsilon_L^3\exp(-5.08\varepsilon_G)$
Velocity	$U_o = U_l + U_g = \varepsilon_l U_l + \varepsilon_g U_g$
Solid phase	
Holdup	$\varepsilon_S + \varepsilon_L + \varepsilon_G = 1$
Velocity	$U_S = 0$
Gas phase	
Holdup	$\frac{U_g}{\varepsilon_G} = \frac{U_g}{1-\varepsilon_S} + \frac{U_l}{1-\varepsilon_S} + 0.1016 + 1.488\left(\frac{U_g}{1-\varepsilon_S}\right)^{0.5}$
Velocity	$U_g = \frac{Q_{g_{out}}}{A_c} = -\frac{d\varepsilon_G H}{dt} + \frac{V}{A_c\rho_G}\sum_{i,j} T_{iG}^j$
Parameters:	
Terminal settling velocity	$U_t = \frac{-17.3\mu_L + [299.29{\mu_L}^2 + 1.344 g {d_{ag}}^3 \rho_L(\rho_S-\rho_L)]^{0.5}}{0.672 d_{ag}\rho_L}$
Expansion coefficient	$n = 4.4Re_t^{-0.1}, \quad 1 < \mathrm{Re}_t < 500$
Phase component mass balance equations	
Liquid phase	$A_c d\frac{\varepsilon_L\phi_{iL}H}{dt} = Q_{l_{in}}\phi_{iL}^* - Q_{l_{out}}\phi_{iL} + V\left(\sum_j R_{iL}^j + \sum_j T_{iL}^j\right), \quad \phi_{iL}^* = \frac{1}{A_c U_o}[Q_f\phi_{iL_f} + Q_r\phi_{iL_{z=H}}], \quad Q_{l_{in}} = Q_o = U_o A_c, Q_{l_{out}} = U_l A_c$
Solid phase	$A_c d\frac{\varepsilon_S\phi_{iS}H}{dt} = V\left(\sum_j R_{iS}^j + \sum_j T_{iS}^j\right)$
Gas phase	$A_c d\frac{\varepsilon_G\phi_{iG}H}{dt} = -Q_{g_{out}}\phi_{iG} + V\left(\sum_j R_{iG}^j + \sum_j T_{iG}^j\right)$

equal to fluid velocity at the reactor inlet ($U_o = U_l + U_g$). The generated gas is assumed to be separated from the multiphase stream at the top of the reactor column, and thus, the gas phase flow rate at the reactor inlet is equal to zero. Since the solid is confined in the control volume, no-flux conditions at the reactor inlet and outlet are assumed. Mass balance equations for phase components have been included in Table B.1.

Appendix C. Nomenclature

A	area
d	diameter
f	biomass composition (fraction)
g	gravity
H	height
I_{COD}	index (g COD mol^{-1})
k	specific rate coefficient, GBWM parameter (Table B.1)
k_La	liquid–gas mass transfer coefficient
K_H	Henry's coefficient
n	expansion coefficient
P, p	pressure
Q	flow rate
R	homogeneous reaction rate
Re	Reynolds number
S	soluble species concentration
T	mass transfer and transport process rate (interface)
V	volume
U	superficial velocity
X	biomass concentration or non-soluble species concentration
z	axial direction

Greeks

ε	phase holdup (volumetric fraction), porosity
η	bed expansion
μ	microorganism growth rate, viscosity (Table B.1)
ν	process rate coefficient
ν_{st}	gas molar volume
ρ	density
ω	specific energy dissipation rate
ϕ	mass or molar concentration

Subscripts

bh	biomass hydrolysis
bp	bioparticle (granule)
c	reactor column
d	biomass death
f	feed
G, g	gas
Hid	hydrolysis
i	phase component index
in	inlet
j	biochemical and physico-chemical process index
L, l	liquid
o	upflow velocity, static bed
out	outlet
r	recycle (flow), rupture (granule)
S	solid
t	terminal
T	total

References

[1] A.W.A. De Man, A.R.M. Van Der Last, G. Lettinga, The use of EGSB and UASB anaerobic systems for low strength soluble and complex wastewaters at temperature ranging from 8 to 30 °C, in: E.R. Hall, P.N. Hobson (Eds.), Proceedings of the Fifth International Conference on Anaerobic Digestion, Bologna, 1988, ISBN 0-08-036634-1, pp. 197–209.

[2] L.W. Hulshoff, S.I. de Castro, G. Lettinga, P.N.L. Lens, Anaerobic sludge granulation, Water Res. 38 (2004) 1376–1389.

[3] G. Lettinga, A.F.M. Van Velsen, S.W. Hobma, W. De Zeeuw, A. Klapwijk, Use of the upflow sludge blanket (USB) reactor concept for biological wastewater treatment, especially for anaerobic treatment, Biotechnol. Bioeng. 22 (1980) 699–734.

[4] I. Angelidaki, L. Ellegaard, B.K. Ahring, A comprehensive model of anaerobic bioconversion of complex substrates to biogas, Biotechnol. Bioeng. 63 (5) (1999) 363–372.

[5] D.J. Batstone, J. Keller, L.L. Blackall, The influence of substrate kinetics on the microbial community structure in granular anaerobic biomass, Water Res. 38 (2004) 1390–1404.

[6] H.Q. Yu, H.H.P. Fang, Acidogenesis of gelatin-rich wastewater in an upflow anaerobic reactor: influence of pH and temperatura, Water Res. 37 (2003) 55–66.

[7] C. Nicolella, M.C.M. Van Loosdrecht, J.J. Heijnen, Wastewater treatment with particulate biofilm reactors, J. Biotechnol. 80 (2000) 1–33.

[8] L. Seghezzo, G. Zeeman, J.B. Van Lier, H.V.M. Hamelers, G. Lettinga, A review: the anaerobic treatment of sewage in UASB and EGSB reactors, Bioresour. Technol. 65 (3) (1998) 175–190.

[9] M. Fuentes, Modeling and dynamic simulation of anaerobic biofilm fluidized bed reactors. Application to the complex effluent treatment, Ph.D. dissertation (in Spanish, ISBN-10: 987-05-0709-3, ISBN-13: 978-987-05-0709-3), Universidad Nacional del Litoral, Santa Fe, Argentina (2006).

[10] A. Rinzema, Anaerobic treatment of wastewater with high concentrations of lipids or sulfate. Ph.D. dissertation, Wageningen Agricultural University, Wageningen, The Netherlands (1988).

[11] Y.H. Liu, Y.L. He, S.C. Yang, C.J. An, Studies on the expansión of the granular bed present in EGSB bioreactors, Water S.A. 32 (2006) 555–560.

[12] A.G. Brito, L.F. Melo, A simplified analysis of reaction and mass transfer in UASB and EGSB reactors, Environ. Technol. 18 (1997) 35–44.

[13] Y. Liu, H.L. Xu, K.Y. Show, JH Tay, Anaerobic granulation technology for wastewater treatment, World J. Microbiol. Biotechnol. 18 (2002) 99–113.

[14] M. Fuentes, N. Scenna, P. Aguirre, M. Mussati, Hydrodynamic aspects in fluidized bed bioreactor modeling, Chem. Eng. Process. 47 (2008) 1530–1540.

[15] M. Fuentes, P. Aguirre, N. Scenna, M. Mussati, Anaerobic biofilm reactor modeling focused on hydrodynamics, Chem. Eng. Commun. 195 (6) (2008) 600–621.

[16] M. Fuentes, P. Aguirre, N. Scenna, M. Mussati, Anaerobic digestion of carbohydrate and protein-based wastewaters in fluidized bed bioreactors, Lat. Am. Appl. Res. 37 (4) (2007) 235–242.

[17] J. Huang, C. Wu, Specific energy dissipation rate for fluidized bed bioreactors, Biotechnol. Bioeng. 50 (1996) 643–654.

[18] M.K. Tiwari, S. Guha, C.S. Harengranath, S. Tripathi, Influence of extrinsic factors on granulation in UASB reactor, Appl. Microbiol. Biotechnol. 71 (2006) 145–154.

[19] S.V. Kalyuzhnyi, V.V. Fedorovich, P. Lens, Dispersed plug flow model for upflow anaerobic sludge bed reactors with focus on granular sludge dynamics, J. Ind. Microbiol. Biotechnol. 33 (2006) 221–237.

[20] L.W. Hulshoff, The phenomenon of granular anaerobic sludge. Ph.D. dissertation, University of Wageningen, The Netherlands (1989).

[21] J.C. Hu, Theory and Technology of Anaerobic Biological Treatment, China Architecture Industrial Publishing Company, Beijing China, 2003.

[22] J. Field. Anaerobic granular sludge bed technology [Online] http://www.uasb.org/discover/granules.htm (2005).

[23] Y.C. Wang, J.E. Zuo, J.H. Xiao, A study on characteristics of anaerobic granular sludge in an EGSB reactor, China Biogas 20 (4) (2002) 3–7.

[24] J.F. Richardson, W.N. Zaki, Sedimentation and fluidization, Part 1, Trans. Inst. Chem. Eng. 32 (1954) 35–53.

[25] V.K. Bhatia, N. Epstein, Three-phase fluidization: a generalized wake model, in: Proceedings of the International Syrup. Fluid. Appl., Cepadues-Editions, Toulouse, 1974, pp. 380–392.

[26] Process Systems Enterprise Ltd., gPROMS Advanced User Guide, Release 2.3, London (2004).

[27] Process Systems Enterprise Ltd., gPROMS Introductory User Guide, Release 2.3.1, London (2004).

[28] R.G. Veronez, A.A. Orra, R. Ribeiro, M. Zaiat, S.M. Ratusznei, J.A.D. Rodrigues, A simplified analysis of granule behavior in ASBR and UASB reactors treating low-strength synthetic wastewater, Braz. J. Chem. Eng. 22 (3) (2005) 361–369.

[29] M.T. Kato, L. Florencio, R.F.M. Arantes, Post-treatment of UASB effluent in an expanded granular bed reactor type using flocculent sludge, Water Sci. Technol. 48 (6) (2003) 279–284.

[30] M. Fuentes, P. Aguirre, N. Scenna, M. Mussati, Application of two anaerobic digestion models to biofilm systems, Biochem. Eng. J. 38 (2) (2008) 259–269.

[31] I. Angelidaki, L. Ellegaarg L., B. Ahring, A mathematical model for dynamic simulation of anaerobic digestion of complex substrates: focusing on ammonia inhibition, Biotechnol. Bioeng. 42 (1993) 159–166.

[32] D.J. Batstone, J. Keller, I. Angelidaki, S.V. Kalyuzhnyi, S.G. Pavlostathis, A. Rozzi, W.T.M. Sanders, H. Siegrist, V.A. Vavilin, Anaerobic Digestion Model No. 1 (ADM1), IWA Task Group for Mathematical Modelling of Anaerobic Digestion Processes, IWA Publishing, London, UK, 2002.

[33] G.I. Efremov, I.A. Vakhrushev, A study of the hydrodynamics of three phase fluidized beds, Int. Chem. Eng. 10 (1970) 37–41.